Non-Ostwald coarsening of the GaAs(001) surface

Wolfgang Braun, Vladimir M. Kaganer, Bernd Jenichen, and Klaus H. Ploog
Paul-Drude-Institut für Festkörperelektronik, Hausvogteiplatz 5-7, D-10117 Berlin, Germany
(Received 16 December 2003; published 9 April 2004)

We study the coarsening kinetics of the two-dimensional island/pit morphology on the GaAs(100) surface after deposition of a fractional layer using grazing incidence x-ray diffraction. We find that the correlation length $l(t)$ increases as $l(t) \propto t^n$, with n in the range 0.7–1.3. For spinodal decomposition (coverage 0.5), we observe linear recovery. Our observations do not fall into the known universality classes of conserved coarsening kinetics, the Lifshitz-Slyozov diffusion-limited kinetics ($l \propto t^{1/3}$), or the Wagner attachment-limited kinetics ($l \propto t^{1/2}$), and therefore cannot be explained by Ostwald ripening. We present experimental results on the coverage, temperature, and orientation dependence of the coarsening rate.

DOI: 10.1103/PhysRevB.69.165405 PACS number(s): 68.43.Jk, 61.10.−i, 81.15.Hi

I. INTRODUCTION

A system brought into a nonequilibrium multidomain state, e.g., by a phase transition in a solid, evolves to increase the size of its individual domains to minimize the interfacial energy. If the fractions of the phases are conserved, the coarsening proceeds by detachment of atoms from smaller islands and attachment to larger islands. This process is called Ostwald ripening. The kinetics of Ostwald ripening is well studied. For reviews, see Refs. 1,2. Remarkably enough, the time evolution is found to be the same in both three dimensions (3D) and two dimensions (2D), and it is independent of the details of the system under consideration. The mean domain size $l(t)$ follows a power law, $l(t) \propto t^n$, with an exponent $n=1/3$ for diffusion-limited kinetics[3] and $n=1/2$ for attachment-limited kinetics.[4]

The classical theory of Ostwald ripening was originally developed for low coverages.[3,4] A number theoretical studies, computer simulations, and experimental investigations have demonstrated its applicability to arbitrary coverages. It is well established that a single mechanism of coarsening, Ostwald ripening, is dominant in the whole range of coverages from 0 to 1, resulting in a coverage-independent time exponent. A number of publications on Ostwald ripening are devoted specifically to the case of spinodal decomposition (coverage 0.5). Let us discuss a few examples.

Marqusee and Ross developed a time scaling scheme and applied it to the diffusion-limited case of Ostwald ripening to show that the coarsening exponent is 1/3, independent of the volume fraction in 3D.[5,6] Marqusee extended this result to the diffusion-limited case in 2D, showing that the coarsening exponent remains 1/3.[7] Mullins derived the results starting from the assumption of statistical self-similarity, without the need for geometrical simplifications or mean-field approximations.[8] Zheng and Gunton included pair correlations and showed that the growth exponent remains 1/3, although the island size distributions are strongly affected.[9] Rutenberg and Bray derived the time exponents through an energy-scaling approach, again confirming an exponent of 1/3 in 2D.[10]

Huse[11] and Roland and Grant[12] investigated Ostwald ripening in the case of 2D spinodal decomposition using Monte Carlo simulations, obtaining exponents approaching 1/3 from below at late times. Yao *et al.* studied Ostwald ripening both analytically and by numerical simulations, finding coarsening exponents of 1/3.[13] Sagui and Desai study the modification of Ostwald ripening by long-range interactions for fractions up to 0.4 in 3D, both analytically and by simulations.[14] The growth exponent is always below 1/3. The recent level set calculations by Petersen *et al.*[15] also reproduced the 1/3 time exponent.

Experimental studies of heteroepitaxial fractional oxygen layers on tungsten by Tringides *et al.*[16] and Wu *et al.*[17] showed a time exponent of less than 1/3 for different coverages between 0 and 1. For 0.5 monolayers (ML) of Cu on Cu(100),[18] growth exponents close to 1/4 are found. Krichevsky and Stavans studied 2D Ostwald ripening in thin layers of succinonitrile with coverages up to 0.54, obtaining an exponent of 1/3.[19,20] Experiments with Langmuir films by Seul *et al.*[21] gave a growth exponent around 0.28 for a coverage of 0.25. Joly *et al.* found classical Ostwald ripening at the late stages of spinodal decomposition in 2D, both experimentally in copolymer thin films and using a qualitative model.[22] Studies of a system close to the current study, the temporal evolution of homoepitaxial 2D islands on Si(100) by Theis *et al.*[23] and Bartelt *et al.*,[24] found the detachment-limited case of Ostwald ripening with a time exponent of 0.5.

The growth conditions in molecular-beam epitaxy (MBE) are usually adjusted so that adatoms can move over long distances and nucleate two-dimensional islands when they meet. During continuous growth, the islands grow, coalesce, and form a continuous layer on which the next layer of islands nucleates. This process is called layer-by-layer growth. In a diffraction experiment, layer-by-layer growth leads to oscillations in the diffracted intensity for diffraction conditions that are sensitive to interference between the beams scattered from different layers. If growth is interrupted at a noninteger layer coverage, the diffracted intensity recovers and the surface returns to its initial state before deposition. It is natural to expect that the recovery proceeds by Ostwald ripening. We would expect a coarsening exponent between the limiting cases $n=1/2$ and $n=1/3$, or somewhat below if the recovery is slowed down, for example, by impurities.

In the present study, we show that the coarsening of 2D islands or pits on the reconstructed GaAs(100)$\beta(2\times4)$ surface proceeds in a qualitatively different way: we observe

coarsening exponents around $n=1$, which means that the mean island size increases approximately *linearly* in time with lateral growth rates around 0.1 nm/s. The experimental verification of this result is based on the direct determination of the mean island/pit size $l(t)$ from the widths of the x-ray diffraction peaks with a simultaneous consistency check using the total integrated intensity. We also determine the coverage, temperature, and in-plane anisotropy of the coarsening rate.

II. EXPERIMENT

The measurements were performed at the PHARAO beamline at the synchrotron BESSY II in Berlin (Germany) in a combined molecular-beam epitaxy/6-circle surface diffractometer system dedicated to the *in situ* x-ray scattering analysis of III-V semiconductor growth;[25] 1 mm thick on-axis GaAs(100) epiready substrates were used. We adjusted the substrate temperature to the center of the stability range of the $\beta(2\times4)$ reconstruction for a rather low As_4 pressure, which was necessary to avoid excessive coating of the Be x-ray windows. This resulted in somewhat lower growth temperatures around 530 °C instead of the widely used 580 °C. Nevertheless, the growth conditions are representative for GaAs MBE, which is demonstrated by the presence of strong intensity oscillations due to layer-by-layer growth with low damping,[26] in agreement with an earlier study using organometallic vapor-phase epitaxy (OMVPE).[27]

The height of an elementary step on a GaAs(100) surface is half of the bulk lattice period. This feature of the zinc-blende structure allows us to perform measurements in a planar grazing incidence—grazing exit geometry.[26] The cubic GaAs unit cell is formed by two layers that are shifted by a relative translation $\mathbf{t}=a[0\,\frac{1}{2}\,\frac{1}{2}]$, where a is the bulk lattice period. A single surface step hence also implies an in-plane translation of $a/2$. The same translation applies to the reconstructed cells on the terraces. Therefore, a reflection $\mathbf{Q}=(2\pi/a)[hkL]$ contains a phase factor of $\exp(i\Phi)$ between the structure amplitudes of the two terraces, where $\Phi=\mathbf{Q}\cdot\mathbf{t}=\pi(k+L)$. In a reflection with odd h and k, the phase factor $\Phi=\pi$ (destructive interference) is obtained in-plane at $L=0$ for terraces separated by single surface steps. In other words, we detect the different terraces by the $a/2$ lateral displacement of the lattice planes instead of their vertical displacement. The 1 3 0 reflection is one of the strongest surface-sensitive in-plane reflections and is therefore used for most of the measurements used in the present study. The incidence and exit angles were just below the critical angle, $L=0.05$.

III. COARSENING AT HALF-LAYER COVERAGE

Figure 1(b) shows the recovery of the diffracted intensity in the 1 3 0.05 reflection after the deposition of 0.5 ML of GaAs. The intensity drops rapidly after deposition as a result of the destructive interference between the two layers of the half-covered surface. The subsequent slow intensity increase is due to the lateral growth of 2D islands/pits: the number of 2D islands/pits which coherently contribute to the diffracted intensity decreases as their size approaches the resolution of the instrument. The relative contribution of destructive interference therefore decreases. Finally, the island size exceeds the resolution limit and each island contributes incoherently.

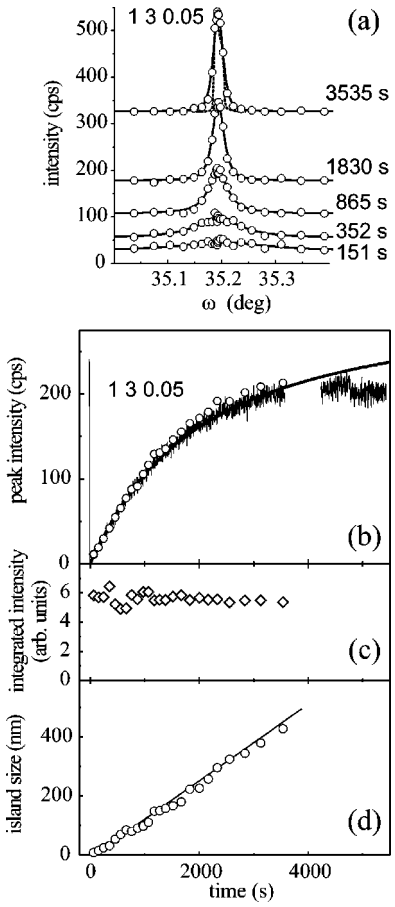

FIG. 1. (a) ω scans of the 1 3 0.05 reflection during recovery after the deposition of 0.5 ML of GaAs. The time at each curve refers to the acquisition of the point at the maximum. The broken line below the top curve is an ω scan of the bulk reflection 220 used to determine the resolution. The curves are Voigt function fits to the experimental data. The curves are shifted vertically for clarity. (b) Time dependence of the peak intensity. The thin black line is the measured peak intensity. Note the initial drop from a value of 240 cps prior to deposition. Circles are the peak intensities obtained from the ω scans during recovery in an independent growth run. The thick gray line is a fit to Eq. (2). (c) Time dependence of the integrated intensity obtained from the Voigt fits. (d) Time dependence of the correlation length $l=2/\Delta q$ obtained from the FWHM's Δq of the Lorentzian components of the Voigt fits. The smallest measured values for l are around 10 nm. Here, as in all subsequent figures, the measured intensity is normalized to a storage ring current of 100 mA and the background is subtracted. The substrate temperature is 530 °C, the As/Ga flux ratio during deposition is 2, and the deposition rate is 0.2 ML/s.

Additional information about the island coarsening can be obtained from ω scans (rocking curves) measured during the recovery, Fig. 1(a). The ω scans are obtained by stepwise rotation of the sample about its normal. Each scan takes approximately 75 s. The ω steps are chosen nonuniformly, with a smaller spacing near the center of the peak, allowing us to

accurately determine the shape both of wide peaks at the beginning of recovery and of narrow peaks as the peak shape approaches a stationary state. The measured peaks are convolutions of an intrinsic peak profile due to islands (or, more generally, surface relief) with the instrumental resolution function. The latter function is obtained by interpolating between the peaks of the 200, 220, and 400 in-plane bulk reflections.[25] The ω scan of the nearest 220 reflection is included in Fig. 1(a) as a broken line. The peak shapes of bulk reflections are close to Gaussian. We therefore use a Gaussian resolution function with the full width at half maximum (FWHM) 0.0155°. The corresponding x-ray coherence length is $l_c = 360$ nm. We find that the measured ω scans are well fitted if we choose a Lorentzian for the intrinsic peak profile. Hence, we fit the measured intensities to a convolution of a Lorentzian and a Gaussian, which is the Voigt function.[28] The Voigt function is used here in the same way as it is usually employed in spectroscopy:[29] the Gaussian width is determined by the instrumental resolution and measured in an independent experiment, while the Lorentzian width is fitted. Then, the number of fit parameters is the same as for a single Lorentzian or a single Gaussian fit to the measured curve. We compare these fits and find that Voigt function fits of the surface reflections give smaller χ^2 values. We therefore conclude that the intrinsic peak profile is Lorentzian, which indicates an exponential correlation function of the 2D structure on the surface. At the coverage $\theta = 0.5$ we consider here, a coherent peak is absent and the Voigt function completely describes the peak shape.

The stationary peak profile measured after sufficiently long recovery gives a mean terrace size of 450 nm, which agrees with *ex situ* atomic force microscopy measurements.[26] We can determine terrace sizes larger than the coherence length because the width of the resolution function is known and any additional contributions to the peak width can therefore be separated. The ability to resolve features larger than the coherence length therefore depends on the accuracy of the raw data. In our case, we additionally benefit from the Lorentzian terrace peak differing in shape from the Gaussian resolution function. The broader wings at its base increase the contrast between the two contributions, allowing an even more reliable separation. The reproducibility of the measurements is demonstrated in Fig. 1(b), where the intensity maxima obtained from the ω scans (circles) are compared to the peak intensity measured in an independent growth run (black curve).

The measurements were performed with a detector acceptance of $\approx 1°$, much larger than the widths of the ω scans in Fig. 1(a). The integrated intensity of a reflection in our measurement is therefore the total intensity of the reflection. According to the kinematical theory of scattering, it is proportional to the total number of unit cells contributing to the scattering. Analyzing a surface requires that the surface reconstruction does not change, which means that the structure factor does not change. For our case, this was shown in a previous study by analyzing the shape of the crystal truncation rods during growth.[26] Since the illuminated area is constant and the penetration depth is fixed by the constant incidence angle of the primary beam, the integrated intensity has to be constant. This is proven by Fig. 1(c), showing that the integrated intensities obtained from the Voigt fits do not change in time. Hence, the constant integrated intensity verifies that we collect all of the relevant intensity. In particular, there is no very broad peak at the beginning of the measurement that we miss due to our finite scanning interval. Figure 1(d) presents the correlation length $l(t) = 2/\Delta q(t)$ obtained from the FWHM $\Delta q(t)$ of the Lorentzian component of the Voigt fits shown in Fig. 1(a). The linear time dependence of the correlation length $l(t)$ on time t is clearly evident from the plot. This is the main result of the present paper. The mean size of the 2D islands/pits increases with a constant rate of $dl/dt = 0.11$ nm/s.

The evolution of $l(t)$ can also be derived from the time dependence of the *peak* intensity $I(t)$ during the initial stage of recovery. The integrated intensity of a Lorentzian peak is $\mathcal{I} = (\pi/2) I(t) \Delta q(t)$. Expressing $\Delta q(t)$ through the correlation length $l(t)$, we have

$$l(t) = \pi I(t)/\mathcal{I}. \tag{1}$$

Knowing that the integrated intensity is constant, we obtain $l(t) \propto I(t)$. For a coverage of 0.5, a measurement of the peak intensity is therefore equivalent to a measurement of the deconvoluted FWHM of the peak.

At later times, the peak intensity $I(t)$ deviates from the linear dependence because of the finite resolution of the diffraction experiment. The peak intensity of the Voigt function, taking into account the resolution, is

$$I(t) = I_0 \exp[(l_c/2l)^2] \operatorname{erfc}(l_c/2l). \tag{2}$$

Here, $\operatorname{erfc}(x)$ is the complementary error function, $I_0 = \mathcal{I} l_c/(2\sqrt{\pi})$ is the peak intensity maximum corresponding to scattering from infinitely large domains, and l_c is the x-ray coherence length. In the limit of $l \ll l_c$, we retrieve Eq. (1). The gray curve in Fig. 1(b) is a fit to Eq. (2) with $l(t) \propto t$.

IV. COVERAGE DEPENDENCE

We have also studied the dependence of the recovery kinetics on the coverage of the top layer. Since the recovery at 1 ML coverage is fast,[26] this coverage serves as a convenient and precise reference point. We therefore varied the deposition times between 0.5 and 1.5 ML instead of between 0.0 and 1.0 ML. Figure 2(a) shows the evolution of the peak profiles after depositing 0.73 ML. Now, the initial peak intensity is higher, since the deposited fractional layer covers more than half of the surface. The measured peak profiles are fitted to curves consisting of two components:[30] a constant resolution-limited coherent contribution represented by the thin solid line and diffuse scattering from 2D islands described by the previously used variable-width Voigt functions (broken lines). The correlation lengths obtained from the Lorentzian components of the Voigt functions for different coverages are shown in Fig. 2(b). The coarsening rates show a distinct asymmetry. The adatom islands (top layer coverage $\theta < 0.5$, which is the deposition of more than 1 ML in our experiment) coarsen faster than the pits (advacancy islands, $\theta > 0.5$). Figure 2(b) indicates that not only the coarsening

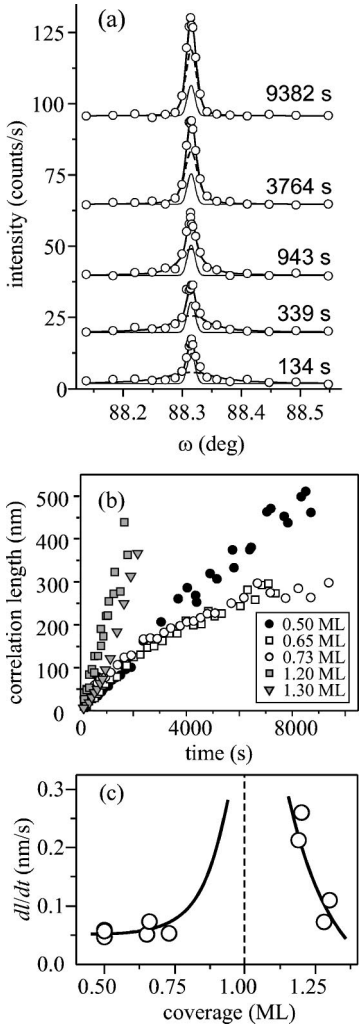

FIG. 2. (a) Time dependence of the diffraction profiles during recovery after the deposition of 0.73 ML of GaAs. For coverages $\neq 0.5$ ML, an additional coherent contribution (thin solid line) is present. (b) Time evolution of the correlation length obtained from fits to diffraction profiles for different coverages. The coarsening rates dl/dt (c) as well as the exponents depend on coverage. Islands grow faster than pits.

rates but also the time exponents depend on the coverage: the exponents are larger than 1 for island coarsening ($\theta < 0.5$) and less than 1 for pit coarsening ($\theta > 0.5$). Our current experimental data are not sufficiently accurate to further analyze the coverage dependence of the exponent. The exponent varies between 0.7 and 1.3. The exponent obtained in several growth runs for a coverage of $\theta = 0.5$ is equal to 1 with an accuracy better than 0.05. The initial slopes dl/dt obtained from the data in Fig. 2(b) are collected in Fig. 2(c). The coarsening rate practically diverges at 1.0 ML coverage, for which we see a complete recovery within as low as 20 s.[31] This is practically instantaneous on the time scale of Fig. 2(b).

V. TEMPERATURE DEPENDENCE AND ANISOTROPY

The coarsening process strongly depends on the substrate temperature, see Fig. 3(a). For these data, the temperature

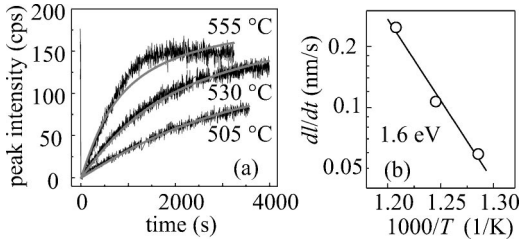

FIG. 3. (a) Time dependence of the peak intensities after deposition of 0.5 ML GaAs at different temperatures. The gray lines are fits using Eq. (2). (b) An Arrhenius plot giving a coarsening activation energy of 1.6 eV.

range is varied within the stability range of the $\beta(2\times4)$ reconstruction. We measure the peak intensities and fit them to Eq. (2). The integrated intensities $\mathcal{I}$ are obtained from ω scans performed prior to each run. Linear coarsening is observed at all three temperatures. The coarsening rates dl/dt obtained at different temperatures are shown in an Arrhenius plot in Fig. 3(b). The slope of the linear fit yields an activation energy of 1.6 eV.

Measurements in different directions along the surface yield an anisotropic coarsening rate, Fig. 4. Normalizing the peak intensities $I(t)$ to the integrated intensities $\mathcal{I}$, Eq. (1), we find that the coarsening is approximately two times slower in the $\bar{3}10$ reflection, compared to the 130 and 110 reflections. The coarsening rates dl/dt are plotted in a polar diagram in the inset of Fig. 4 for the three measured directions (empty circles) and the ones related by the symmetry operations about the 110 and $1\bar{1}0$ axes (full circles). The shaded rectangle serves as a guide to the eye. Note that the ω rocking scans probe the ordering *perpendicular* to the scattering vector. The Miller indices of a reflection therefore differ from the corresponding vector in the polar diagram. The coarsening rate in the $[1\bar{1}0]$ direction is about twice the rate

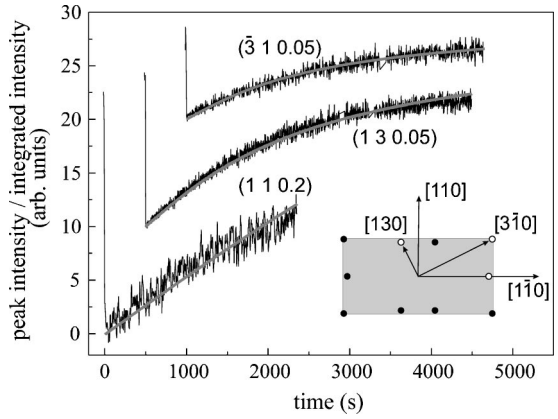

FIG. 4. Time dependence of the peak intensities in different in-plane directions normalized by the corresponding integrated intensities $\mathcal{I}$; 0.5 ML GaAs is deposited at 530 °C. The curves are shifted both vertically and horizontally for clarity. The gray lines are fits using Eq. (2). The inset shows a polar plot of the measured coarsening rates dl/dt in real space. Empty circles denote the measured values and full circles correspond to the ones obtained by reflections about the [110] and $[\bar{1}10]$ symmetry axes.

along [110], which agrees well with the anisotropic islands observed by real-space methods.[33–35] The island aspect ratio of 2 does not change in time, since the growth proceeds at a constant rate.

VI. DISCUSSION

Our experimental results disagree with classical Ostwald ripening in two decisive points: first, we observe coarsening exponents well above 0.5; second, we observe an exponential correlation function of the islands/pits on the surface.

The coarsening kinetics of 2D islands on the GaAs(100)$\beta(2\times4)$-reconstructed surface does not fall into one of the classes of conserved coarsening kinetics.[1–4] The exponent $n=1$ obtained in our x-ray diffraction experiments is unexpectedly large. The deviation from the expected behavior therefore cannot be attributed to imperfections. Such imperfections could explain exponents below the expected values since they would most probably slow down the coarsening process. Instead, our values are too high. It is also worth noting that as we approach the original validity range of the classical Ostwald model at low coverages, the coarsening exponent deviates to even larger values above 1 instead of approaching the expected values. The observed discrepancy with classical Ostwald ripening can therefore not be explained by an attempt to apply a model well outside its validity range.

We have used the same type of measurements and data processing in an investigation of the nonconserved coarsening kinetics of surface reconstruction domains on GaAs(100).[31] The measurements were performed in part on the same samples in alternating sequence with the ones shown here. The diffraction conditions were the same, differing only in the choice of fractional-order (superlattice) reflections instead of the integer reflections used in the present work. We found coarsening exponents distinctly smaller than in the present study, $n=0.22\pm0.05$ and $n=0.42\pm0.05$. This indicates that the island coarsening mechanism is qualitatively different from reconstruction domain coarsening on the same surface.

The adatom islands (top layer coverage $\theta<0.5$) coarsen faster than the pits (advacancy islands, $\theta>0.5$). This is possibly due to a larger adatom attachment energy at concave steps (pit boundaries) compared to convex steps (island boundaries). In addition, we do not expect mobile advacancies on the surface. Material transport in the case of pit coarsening should therefore also take place by adatom migration. This implies that atoms moving from one pit to the next have to detach from the pit edge to the terrace surrounding the pit, a process that may be energetically more expensive or may have a smaller rate than detachment into the pit.

The various models of coarsening typically produce values for the time exponent that are fractions of small integers. It is therefore remarkable that we observe a coarsening exponent very close to 1 at $\theta=0.5$, deviating systematically to larger values for lower coverages and smaller values for higher coverages. We speculate that this may be related as well to the curvature of the steps (island/pit boundaries) on the surface. For coverages somewhere below 0.5, the average curvature of the steps (adatom island boundaries) on the surface is positive (convex) and somewhere above 0.5 (advacancy island boundaries) it is negative (concave). The limiting case in between has similarities with a (stretched) checkerboard pattern, and the steps on average are straight. We therefore speculate that we do not have two competing processes with time exponents above and below 1 that coincidentally balance to 1 at $\theta=0.5$, but instead a single process with a curvature dependence. This process at $\theta=0.5$ may constitute another generic or limiting case similar to the 1/3 and 1/2 time exponents of classical Ostwald ripening.

The activation energy of 1.6 eV we find for the coarsening process agrees with the activation energy of 1.58 eV for adatom diffusion on the GaAs(100) surface obtained from reflection high-energy electron diffraction oscillations.[32] Diffusion-limited Ostwald ripening, however, results in an exponent of 1/3, even below the 1/2 expected for the attachment/detachment-limited case. It is therefore not obvious which elementary process is characterized by this activation energy.

A constant growth rate is typical for crystal growth from a supersaturated solution, in which the shape of the crystal approaches a self-similar shape.[38] This is consistent with the results shown in Fig. 4. In such a scenario, however, a reservoir of Ga atoms is needed to provide the supersaturated surrounding for the growing islands. If we continue growth past the fractional coverage in our experiment, we observe layer-by-layer growth with a constant period in the diffraction signal.[26] Therefore, the deposited Ga atoms are incorporated into the growing GaAs crystal and it is unlikely that a Ga reservoir is established from the atoms supplied by the Ga beam. If such a reservoir existed anyway, we would observe a change in coverage during recovery. However, the fits are consistent with a constant coverage, see Figs. 1(a) and 2(a).

In our fits to the diffraction profiles, we consistently obtain Lorentzian peak profiles. This is a remarkable result, since it implies an exponential island/pit distribution, something which is not expected for classical Ostwald ripening. The universal size distribution[3] of Ostwald ripening is sharply peaked at the mean island size, which would lead to split diffraction peaks with a peak separation comparable to the peak width, in contradiction to our observations.

In this context, it is worth to compare our results to the previous x-ray studies on Ag homoepitaxy[39,40] and on the growth of GaAs by OMVPE.[27] These studies measure the peak profiles during deposition and find side maxima at $\theta=0.5$ during growth. This is not necessarily contradicting our results, since the surface kinetics during growth are dominated by nucleation and coalescence instead of coarsening. The time scale for this process is three to four orders of magnitude smaller than the recovery studied here. It is therefore likely that nucleation and coalescence are governed by a mechanism different from the one at work during coarsening.

One may think that kinetic limitations due to the low growth temperature destroy the island-island correlations typical for Ostwald ripening in our experiments, thus leading to the observed unsplit peak profiles during recovery. We are, however, working in a regime where we observe strong dif-

fraction oscillations with low damping if we continue growth past the fractional coverages discussed here.[26] This means that we have almost perfect layer-by-layer growth with high surface mobility. Fuoss *et al.*[27] found a similar behavior in OMVPE growth: the oscillations with low damping persist down to 520 °C substrate temperature, where the growth becomes limited by the incomplete cracking of the precursor, leading to an increased period of the oscillations. To verify that the deposition kinetics do not affect our results, we have also studied the recovery after growing several layers, stopping growth at 8.5 ML coverage instead of 0.5 ML. We obtain the same exponent $n=1$ in both cases. Both the OMVPE study on GaAs as well as the works on Ag homoepitaxy do not follow the recovery long enough to deduce a coarsening exponent. The initial recovery data shown, e.g., in Fig. 1 of Ref. 27 are sufficiently similar to our results, not to rule out linear recovery for OMVPE as well. One has to keep in mind, though, that the unknown kinetics of the precursor decomposition at the surface as well as significant flux transients, especially at the termination of growth, complicate a direct comparison of OMVPE with MBE experiments.

The classical theory of Ostwald ripening is based on a very limited number of assumptions and therefore describes a wide range of systems. This is most probably the reason for its universal applicability. On the other hand, this means that there is not much room for modifications of the model to produce larger exponents. One of the results of the theory[1–4] is the existence of only one relevant length scale in the system, which in our case would be the average island size. We have already seen that a peaked island size distribution is not present in our experiments. The theoretical models assume that the chemical potential difference inside and outside the island is proportional to the curvature of the island boundary (Gibbs-Thompson pressure). It is not obvious why this assumption should not be true in our case. The crystal growth of compound semiconductors, however, differs from the growth of elemental semiconductors in that the chemical potential of at least one of the constituent elements can be pinned. In the case of GaAs MBE, this is done by fixing the As_4 pressure. This has been suggested as a possible reason for the unexpectedly large density of adatoms observed on the GaAs(100) surface.[36] The equilibrium with the As_4 beam may modify the energy of adatom detachment from the step edge,[37] but there is no obvious reason why this should affect the coarsening exponent. Apart from that, the activation energy of 1.6 eV obtained in the present work is notably smaller than the activation energy deduced in these adatom density studies.[36,37] The fact that a coarsening exponent of 1/2 is observed for Si(100) (Refs. 23,24) may indicate, however, that the mechanism responsible for linear coarsening is specific to compound crystal growth.

VII. SUMMARY

In conclusion, the coarsening kinetics of 2D islands/pits on the GaAs(100)$\beta(2\times4)$ reconstructed surface does not fall into one of the universality classes of conserved coarsening kinetics,[1–4] showing distinctly larger time exponents n from 0.7 to 1.3. The exponent is remarkably close to 1 for half-layer coverages. Since the most closely related system, 2D epitaxial islands on Si(100),[23,24] has been shown to yield $n=1/2$, we speculate that the origin for this exotic behavior is specific to compound semiconductor growth.

ACKNOWLEDGMENTS

The authors would like to thank D. K. Satapathy and X. Guo for assistance in the measurements.

[1] A.J. Bray, Adv. Phys. **43**, 357 (1994).
[2] O.G. Mouritsen, in *Kinetics of Ordering and Growth at Surfaces*, edited by M. G. Lagally (Plenum Press, New York, 1990), p. 1.
[3] I.M. Lifshitz and V.V. Slyozov, J. Phys. Chem. Solids **19**, 35 (1961).
[4] C. Wagner, Z. Elektrochem. **65**, 581 (1961).
[5] J.A. Marqusee and J. Ross, J. Chem. Phys. **79**, 373 (1983).
[6] J.A. Marqusee and J. Ross, J. Chem. Phys. **80**, 536 (1984).
[7] J.A. Marqusee, J. Chem. Phys. **81**, 976 (1984).
[8] W.W. Mullins, J. Appl. Phys. **59**, 1341 (1986).
[9] Q. Zheng and J.D. Gunton, Phys. Rev. A **39**, 4848 (1989).
[10] A.D. Rutenberg and A.J. Bray, Phys. Rev. E **51**, 5499 (1995).
[11] D.A. Huse, Phys. Rev. B **34**, 7845 (1986).
[12] C. Roland and M. Grant, Phys. Rev. B **39**, 11 971 (1989).
[13] J.H. Yao, K.R. Elder, H. Guo, and M. Grant, Phys. Rev. B **47**, 14 110 (1993).
[14] C. Sagui and R.C. Desai, Phys. Rev. Lett. **74**, 1119 (1995); Phys. Rev. E **52**, 2822 (1995).
[15] M. Petersen, A. Zangwill, and C. Ratsch, Surf. Sci. **536**, 55 (2003).
[16] M.C. Tringides, P.K. Wu, and M.G. Lagally, Phys. Rev. Lett. **59**, 315 (1987).
[17] P.K. Wu, M.C. Tringides, and M.G. Lagally, Phys. Rev. B **39**, 7595 (1989).
[18] H.-J. Ernst, F. Fabre, and J. Lapujoulade, Phys. Rev. Lett. **69**, 458 (1992).
[19] O. Krichevsky and J. Stavans, Phys. Rev. Lett. **70**, 1473 (1993).
[20] O. Krichevsky and J. Stavans, Phys. Rev. E **52**, 1818 (1995).
[21] M. Seul, N.Y. Morgan, and C. Sire, Phys. Rev. Lett. **73**, 2284 (1994).
[22] S. Joly, A. Raquois, F. Paris, B. Hamdoun, L. Auvray, D. Ausserre, and Y. Gallot, Phys. Rev. Lett. **77**, 4394 (1996).
[23] W. Theis, N.C. Bartelt, and R.M. Tromp, Phys. Rev. Lett. **75**, 3328 (1995).
[24] N.C. Bartelt, W. Theis, and R.M. Tromp, Phys. Rev. B **54**, 11 741 (1996).
[25] B. Jenichen, W. Braun, V.M. Kaganer, A.G. Shtukenberg, L. Däweritz, C.-G. Schulz, K.H. Ploog, and A. Erko, Rev. Sci. Instrum. **74**, 1267 (2003).
[26] W. Braun, B. Jenichen, V.M. Kaganer, A.G. Shtukenberg, L. Däweritz, and K.H. Ploog, Surf. Sci. **525**, 126 (2003).
[27] P.H. Fuoss, D.W. Kisker, F.J. Lamelas, G.B. Stephenson, P. Imperatori, and S. Brennan, Phys. Rev. Lett. **69**, 2791 (1992).

[28] See Eric Weisstein's World of Science, http://scienceworld.wolfram.com/physics/VoigtLineshape.html
[29] B.H. Armstrong, J. Quant. Spectrosc. Radiat. Transf. **7**, 61 (1967).
[30] C.S. Lent and P.I. Cohen, Surf. Sci. **139**, 121 (1984).
[31] V.M. Kaganer, W. Braun, B. Jenichen, L. Däweritz, and K.H. Ploog, Phys. Rev. Lett. **90**, 016101 (2003).
[32] J. Neave, P. Dobson, B. Joyce, and J. Zhang, Appl. Phys. Lett. **47**, 100 (1985).
[33] T. Ide, A. Yamashita, and T. Mizutani, Phys. Rev. B **46**, 1905 (1992).
[34] J. Sudijono, M.D. Johnson, C.W. Snyder, M.B. Elowitz, and B.G. Orr, Phys. Rev. Lett. **69**, 2811 (1992).
[35] J. Sudijono, M.D. Johnson, M.B. Elowitz, C.W. Snyder, and B.G. Orr, Surf. Sci. **280**, 247 (1993).
[36] M.D. Johnson, K.T. Leung, A. Birch, B.G. Orr, and J. Tersoff, Surf. Sci. **350**, 254 (1996).
[37] J. Tersoff, M.D. Johnson, and B.G. Orr, Phys. Rev. Lett. **78**, 282 (1997).
[38] A. Pimpinelli and J. Villain, *Physics of Crystal Growth* (Cambridge Universtity Press, Cambridge, 1998), p. 62.
[39] H.A. Van der Vegt, W.J. Huisman, P.B. Howes, and E. Vlieg, Surf. Sci. **330**, 101 (1995).
[40] J. Alvarez, E. Lundgren, X. Torrelles, and S. Ferrer, Phys. Rev. B **57**, 6325 (1998).